Thermal Conductance in Spotwelded Titanium Joints

J. N. NYLANDER,* R. R. JUNE,† AND J. B. KELLY*
The Boeing Company, Renton, Wash.

An analytical and experimental study has been made of thermal conductance at material interfaces in spotwelded 8Al-1Mo-1V titanium alloy. Finite-difference techniques were used to predict the thermal conductance at the interface. Results of the analysis and experiment were used to compare temperature and thermal stress distributions in typical skin-z-stiffener sections for assumed perfect thermal contact and the more realistic case of a finite thermal conductance at the interface. It was found that the thermal conductance decreases with increasing material thickness and increases with increasing temperature.

Introduction

HIGH-SPEED aircraft subjected to aerodynamic heating experience structural temperature distributions that are dependent upon the material, geometry, and manner in which the structure is fabricated. The purpose of this paper is to examine the effects of spotwelded joints in 8Al-1Mo-1V titanium alloy on the temperature distribution and the induced thermal stresses arising from nonuniform temperature conditions in such structures.

The problem of contact resistance to heat transfer is not new. The complexity of the geometry and boundary conditions at the interface has precluded rigorous analytical solution. Use of thin material thicknesses in high-temperature areas requires consideration of thermal buckling in addition to strength requirements. For this reason, more precise data and analysis techniques are required in order to predict the temperature and thermal stress distributions resulting from aerodynamic heating of tne structure.

The extensive use of spotwelding in aircraft structures as a means for joining materials to be subjected to high temperatures is relatively new; the majority of available design data is concerned with the contact resistance associated with riveted or bolted joints. In addition, the increasing promise of new high-temperature structural materials, such as titanium, requires experimental verification of contact resistance analyses made for such materials.

Previous work on thermal contact resistance can be divided into two general categories. The first category includes work concerned with a detailed mathematical description of a model representing the geometry and processes occurring at the interface, and solution of the resulting boundary value problem. This approach is typified by the work of Fenech and Rohsenow,[1] Cetinkale and Fishenden,[2] and Laming.[3] The second category indicates work devoted to development of design data for particular joints in specific materials and includes the extensive experimental studies by Barzelay, et al.[4–9]

The approach of the present paper is to obtain a macroscopic description of the processes occurring at the interface through normally available engineering information relative to interface surface condition and geometry. The results of finite-difference solutions for the temperature distribution in spotwelded sheets of 8Al-1Mo-1V titanium alloy of various thicknesses are compared with experimental data. Also shown are analytical results for temperature and thermal stress distributions in a typical skin-stringer configuration comparing the perfect contact and contact resistance cases.

Received September 8, 1964; revision received February 25, 1965.

* Associate Research Engineer, Structures Staff, Airplane Division.

† Unit Chief, Structures Staff, Airplane Division. Member AIAA.

Analysis

Finite-difference solutions to the heat-conduction equation have been used successfully in many aerospace structural applications for predicting transient temperature distributions in complex geometries subject to given heating rates or prescribed boundary temperatures. The method used in the present study is similar to that of Dusinberre[10] and has been incorporated into a digital computer program known as the Boeing Thermal Analyzer.[11] This program is capable of determining transient or steady-state temperature distributions in three-dimensional structures taking into account the effects of conduction, radiation, convection, and variable material properties. The use of this program requires division of the structure into a group of nodes and subsequent representation as a thermal network.

Figure 1 shows the idealization of a spotwelded joint with volume elements. The corresponding thermal network is shown in Fig. 2. It was assumed that the thermophysical properties of the weld nugget and the heat affected zone in the vicinity of the nugget were the same as the base material. It was further assumed that the temperature distribution in the vicinity of the weld was symmetrical in the plane of the plates. Other assumptions that were employed were that a uniform heat flux was received by one face and rejected by the other, and that no heat was transferred across the edges of the plates. As in any numerical solution, the results obtained are dependent upon the nodal network chosen. A total of 35 nodes was used in the present analysis. The modes of heat transfer considered were 1) conduction through the air gap between the plates, 2) conduction through the spotweld, 3) radiation across the air gap, and 4) lateral conduction within the plates.

In compiling the numerical data for the finite-difference solution, it was necessary to make an estimate of the air gap

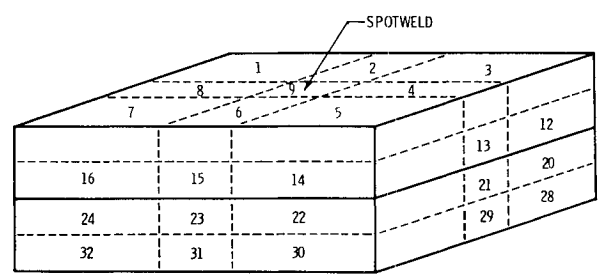

Fig. 1 Idealization of a spotwelded joint with volume elements.

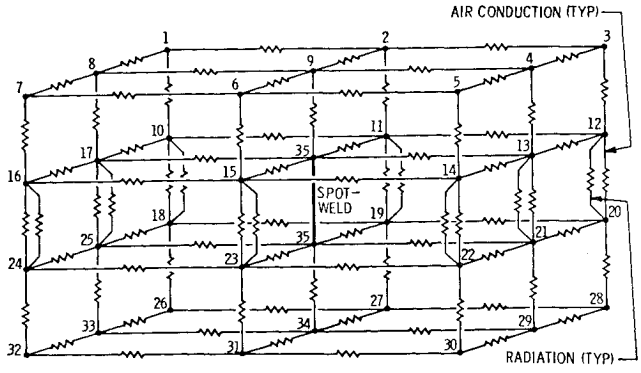

Fig. 2 Thermal network representation of a spotwelded joint.

thickness in the spotwelded joint. A relationship between equivalent air gap thickness, maximum height of surface asperities, and the ratio of actual contact surface to the total surface is given by Shlykof, Ganin, and Demkin[12] as

$$\delta_{eq} = h_{max}(1 - \epsilon)^2/2$$

where δ_{eq} = equivalent gap thickness, h_{max} = maximum height of surface asperity, and ϵ = ratio of actual contact area to total area.

The root-mean-square surface roughness of "as rolled" titanium in thin sheets is about 10 μ. If it is assumed that the distribution of the roughness is Gaussian, peak values range from about three to ten times the root-mean-square value. Also, for "as rolled" surfaces, $\epsilon \ll 1$, and the equivalent gap thickness can be approximated by

$$\delta_{eq} \simeq h_{max}/2$$

This leads to equivalent air gap thicknesses ranging from 0.0005 to 0.002 in. These values do not take into account the physical behavior encountered in welding thin material, such as warpage and material forge-out in the vicinity of the spotweld.

To arrive at an effective joint conductance, the steady-state temperature drop (ΔT) through the welded plates was found. An over-all heat-transfer coefficient was then defined as

$$h_0 = q/\Delta T$$

where q is the heat flux through the structure. For the case of perfect contact between the plates,

$$h_0 = h_{pc} = k/2t$$

where k = thermal conductivity of titanium, and t = plate thickness. The effective joint conductance ($\bar{h}$) was then defined by the relationship

$$1/\bar{h} + 1/h_{pc} = 1/h_0$$

or

$$\bar{h} = h_{pc}h_0/(h_{pc} - h_0)$$

Experiment

Apparatus

The apparatus used in the experimental portion of this study can be considered to be made up of three major components: 1) the specimen holder and heating system, 2) the heating controller, and 3) the temperature recording system.

The specimen holder and heating system, in turn, consists of the specimen holder, the metering blocks, the specimen, a cooling nozzle, and the infrared heating lamps. A view of this portion of the apparatus is shown in Fig. 3, and it was built up as follows. A slab of transite was set upon firebricks, which were placed on edge. A 7-in. square hole was cut in the transite to accommodate the specimen and metering blocks, which were each 6 in. square. During the test, the lower metering block rested on the edges of the two rows of firebrick, and the specimen rested on the lower metering block with the upper metering block on top of the specimen; a silver paint‡ was applied between the specimen and both metering blocks to improve the thermal contact. The void between the specimen and metering blocks and the transite was packed with insulation to minimize edge losses. Eight parallel 12-in. tungsten-filament infrared lamps were suspended about 4 in. above the transite slab and surrounded by a wall of firebrick, forming a partial enclosure. The cooling nozzle was placed under the transite slab and aimed at the lower metering block to provide a continuous flow of cooling air. The 100-psi plant-air system was the source of air for the nozzle.

The heating controller was basically a Boeing Model EHL-1 temperature controller and a Research Inc. Thyratron Power Regulator, Model 8057. This controller received a signal from a thermocouple attached to a thin stainless-steel plate placed under the heating lamps. A constant temperature was

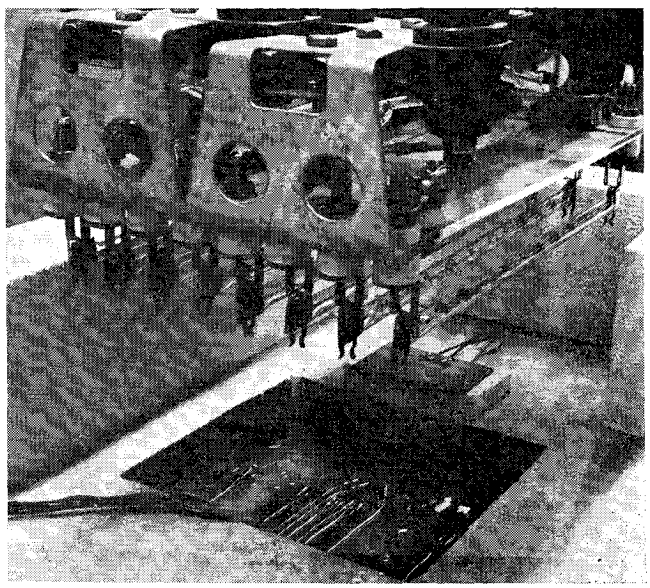

Fig. 3 Close-up view of apparatus showing specimen holder and heating lamps (specimen in place).

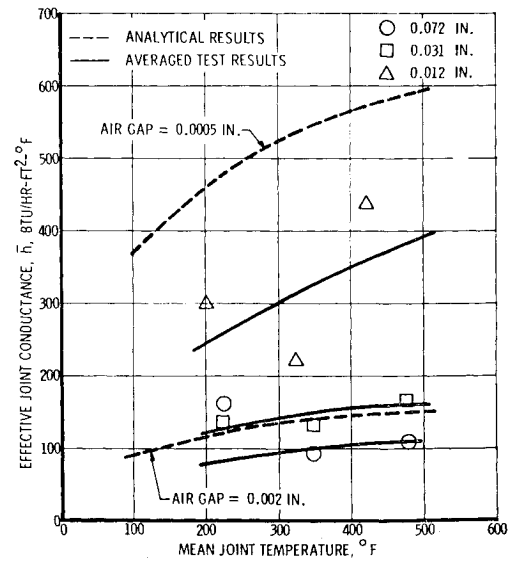

Fig. 4 Variation of effective joint conductance with joint temperature.

‡ Number 21-1 Silver Print, from the GC Electronics Co., Los Angeles, Calif., and Rockford, Ill.

maintained on this plate, thus providing a constant heating rate to the specimen and metering blocks.

The instrumentation consisted of 18 thermocouples, nine each in the two metering blocks. In each metering block, temperature gradient through the block was measured by two sets of three thermocouples each, installed in the space of 0.375 in. One set was located in the center of the block, with the other offset by 1.0 in. The remaining three thermocouples were used to obtain an indication of the importance of edge losses. The outputs of these thermocouples were fed through two stepping switches and a reference junction at 32°F and monitored on two Non-Linear Systems Model V60C digital voltmeters. In addition, one of these thermocouples was continuously recorded on a chart recorder to give an indication of when the system was approaching a steady-state condition.

Test Specimens

Nine 6- by 6-in. test specimens were manufactured, giving all possible combinations of three material thicknesses and three spotweld patterns. The thicknesses used were 0.012, 0.031, and 0.072 in., and the three spotweld patterns gave 4, 9, and 36 spotwelds per specimen, spaced uniformly over the surface.

Test Procedure

Testing was conducted in the following manner. One coat of silver paint was applied to the metering blocks and both sides of the specimen. They were then placed together and set in the specimen holder, and heat was applied until the specimen reached approximately 400°F, at which time the lamps were turned off, and the cooling air was started. After cooling to near-ambient temperature, the specimen and metering blocks were removed and separated. The painted surfaces were brushed lightly, and a second coat of silver paint was applied. The metering blocks and specimen were reassembled and placed in the specimen holder. At this point, the heating lamps and cooling air were both turned on with the heating controller set to bring the specimen to a temperature of approximately 200°F. The nozzle was set at the maximum air flow in order to obtain maximum thermal gradients. All thermocouple readings were recorded at steady-state conditions. This procedure was repeated at temperatures of 350° and 450° to 500°F. The variation in the high-temperature point was due to the varying specimen conditions and represented the maximum practical temperature attainable with this apparatus.

Data Reduction

After testing was complete, the metering blocks were cut to determine precise locations of all thermocouples. Test data were reduced by computing an average heat flux through

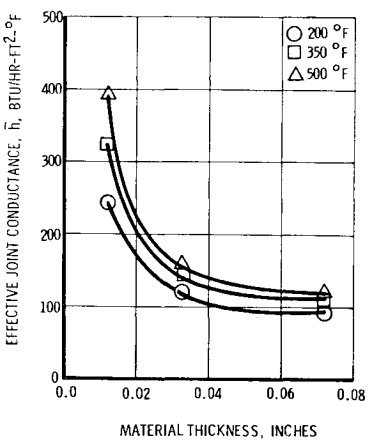

Fig. 5 Variation of effective joint conductance with material thickness.

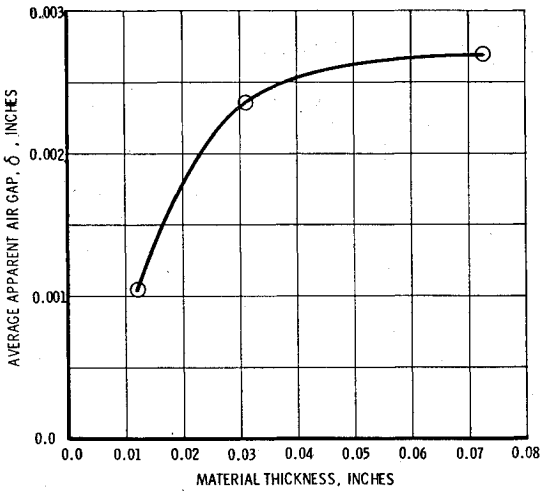

Fig. 6 Effective air gap of spotwelded joint for varying material thickness.

the metering blocks based on the temperature gradient measurements from each test run. The metering blocks were made of the same material as the specimen. This allowed the simplification of the data reduction equations to the point where the effective joint conductance ($\bar{h}$) was expressed as the thermal conductivity of the material multiplied by a function of the measured temperatures and dimensions of specimen and metering blocks. Therefore, a given percentage error in the conductivity would have resulted in an identical percentage error in the effective joint conductance. The values of thermal conductivity used in this study ranged (approximately linearly) from 0.82×10^{-4} Btu/sec-in.-°F at 100°F to 1.28×10^{-4} Btu/sec-in.-°F at 600°F. To obtain the temperature drop across the specimen, it was necessary to correct the total temperature drop for the effects of the layers of silver paint on each side of the specimen. This was done by using the results of several test runs that employed only the metering blocks and one layer of silver paint. A curve of temperature drop through the paint as a function of heat flux was developed. This curve was then used to determine the temperature drop across the test specimen. Combining the heat flux and the temperature drop across the specimen

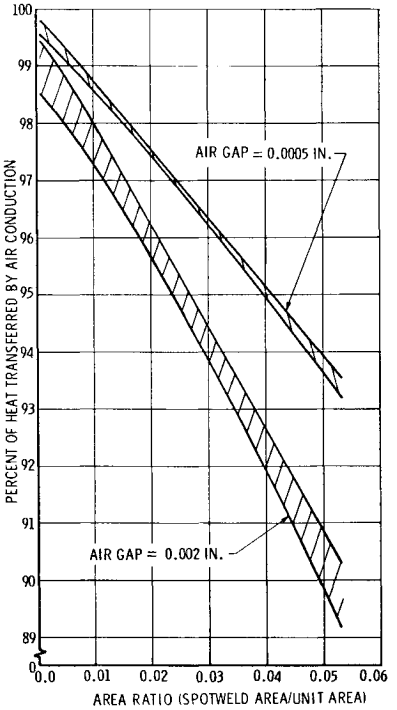

Fig. 7 Percentage of heat conducted through the air in spotwelded joints.

yielded an effective over-all conductance (h_0), which was then reduced to obtain the conductance across the air gap ($\bar{h}$). From the values of air gap conductance, an apparent air gap thickness ($\bar{\delta}$) was found, where $\bar{\delta} = k_a/\bar{h}$, and k_a is the thermal conductivity of air.

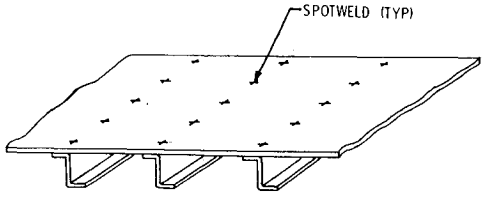

Fig. 8 Typical skin-z-stiffener structure.

Results

In general, good agreement was obtained between analytical and test values for the effective joint conductance. In both cases, it was found that effective joint conductance ($\bar{h}$) increased with increasing temperature, as shown in Fig. 4. It should be noted that the test values at about 200°F appear to be consistently high. It is felt that this was the result of the small temperature differences that were being measured, especially in the thin specimens. The values shown appear high because, as the temperature difference approaches zero, an over-all conductance equal to perfect contact is approached. This condition did not occur at higher temperature levels or for the thicker samples. The temperature drop in each metering block varied from 10°F for the 200°F test condition to 40°F for the 500°F test condition. It is believed that temperatures were measured with an accuracy of ±1°F. The edge losses were found to be negligible for all test conditions. Since it is believed that the joint conductance increases with temperature, and that because of the "forge-out" phenomenon the joint conductance decreases with increasing material thickness, the experimental curves in Fig. 4 were drawn as members of the same family as the analytical results. Figure 5 shows smoothed curves of effective joint conductance as a function of material thickness for the test temperatures. The forge-out phenomenon is the result of the spotwelding process. As the spotweld is formed, parent material is forged between the two plates, forcing them apart. It is felt that the higher rigidity of the thicker specimens causes this gap to be sustained over more of the specimen area, thus causing the increase in apparent air gap. This effect may also be related to the number of spotwelds per unit area, but the test data were inconclusive on this point. Taking into account the variation of the thermal conductivity of air with temperature, the average apparent air gap ($\bar{\delta}$) was found to be a function of material thickness but not temperature, as shown in Fig. 6.

The analytical results also showed that the mode of heat transfer was largely air conduction. For the various area ratios considered (spotweld area per unit area), the air conduction varied from 89.2 to 99.8% whereas the radiation accounted for a maximum of 1.37% of the total heat transferred at a mean spotweld temperature of 500°F. The amount of heat conducted through the spotweld varied from a minimum of 0.09% to a maximum of 10.5%. Figure 7 shows the percent of heat conducted through the air for various area ratios. Since the mean spotweld temperature had a very limited effect upon these values, the figure shows two bands of results for the two air gap thicknesses with each band encompassing all temperatures that were considered.

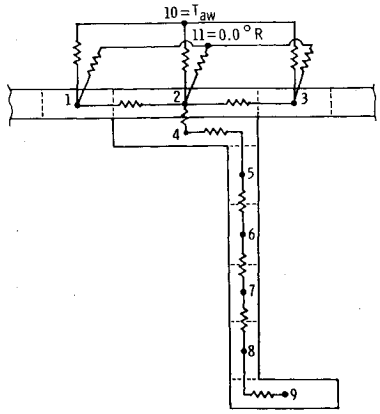

Fig. 9 Thermal network representation of skin-z-stiffener structure.

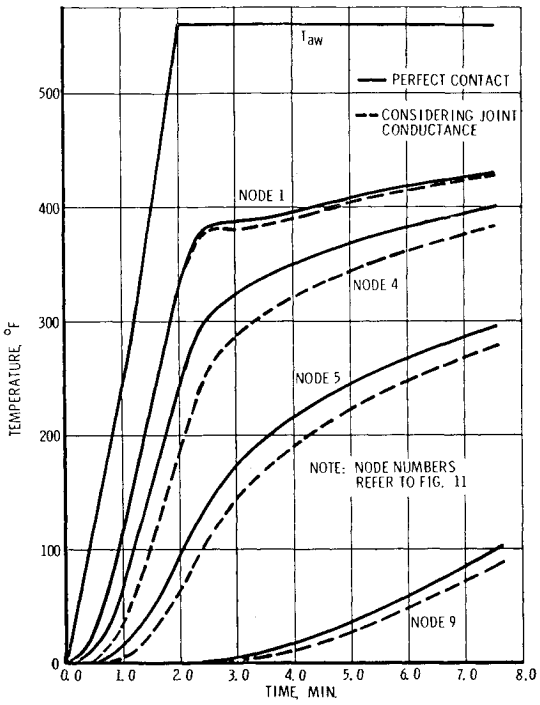

Fig. 10 Transient temperatures in a 0.125-in. skin-z-stiffener.

Application to Typical Structures

The effects of the thermal contact resistance of spotwelded joints on temperature and thermal stress distributions in aircraft structures were studied by analyzing the typical

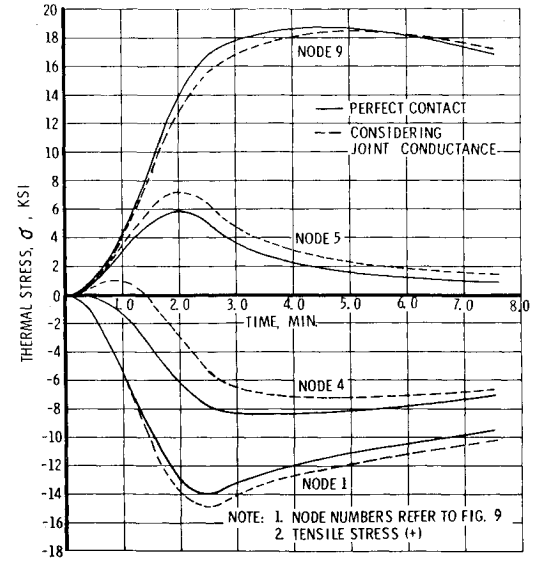

Fig. 11 Transient thermal stresses in a 0.125-in. skin-z-stiffener.

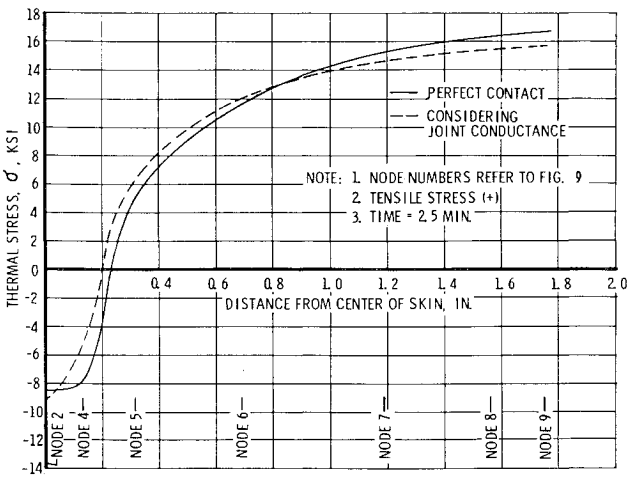

Fig. 12 Stress distribution in a 0.125-in. skin-z-stiffener.

skin-z-stiffener configuration shown in Fig. 8. The thermal network for a typical segment of this structure is shown in Fig. 9. It was assumed that no heat flow occurred parallel to the stiffener, and radiation in the interior of the structure was neglected. The skin surface was given an incident heat flux corresponding to the acceleration portion of the trajectory of a typical Mach 3 aircraft; reradiation to outer space was also considered. In order to show the effects of the thermal conductance of the spotwelded joint, two cases were studied. The first case assumed perfect thermal contact between skin and stiffener. In the second case, an effective joint conductance ($\bar{h}$), based on experimental results, was used. It was found that the effect of joint conductance increased in significance as the thickness of the welded material increased. For this reason, the results shown are for 0.125-in. material, where the effective joint conductance was obtained by extrapolation of Fig. 5.§

Figure 10 shows the transient temperature response of selected nodes for the two cases under consideration. It can be seen that the temperature at node 4, or just below the spotwelded joint, was the most affected by the use of a finite joint conductance. The transient thermal stresses shown in Fig. 11 were computed with the structure represented as a long beam, free to expand without end rotation. A comparison of the stress distributions in the structure at a given time in the trajectory is shown in Fig. 12.

Concluding Remarks

Comparison of the analytical and experimental results showed reasonable agreement, particularly in light of the fact that effects of the manufacturing process were not considered in the analysis. Another area of agreement between analysis and experiment was the finding that the effective joint conductance increased as the mean joint temperature increased. An important point that was not predicted by the theoretical analysis, but appeared in the experimental results, was that the apparent air gap increased with increasing thickness of welded material. In addition, the theoretical analysis showed that conduction through the air was the dominant mode of heat transfer in the joint, amounting to 89% or greater for the cases considered. A related effect was that radiation across the air gap was negligible at least up to joint temperatures of 500°F.

The results of the analysis on the effect of joint conductance on skin-z-stiffener structures led to the conclusion that this effect should be taken into consideration in the design of the structure. Based on the results of this investigation, particularly the effect of material thickness on apparent air gap, it is recommended that the study be extended using material of greater thickness. Also, since many aircraft structures require the joining of unequal thickness material, some investigation should be undertaken on spotwelded joints of this type.

§ As part of a continuing program on titanium technology, measurements were made of the effective joint conductance of a skin-z-stiffener with a 0.15-in. skin thickness and a 0.2-in.-thick stiffener. The results verify the extrapolation of Fig. 5 made for this analysis. Because of the gradual slope of the curves at this thickness, the effects of unequal material thicknesses were minimal.

References

[1] Fenech, H. and Rohsenow, W. M., "Prediction of thermal conductance of metallic surfaces in contact," J. Heat Transfer, **85**, 15–24 (1963).

[2] Cetinkale, T. N. and Fishenden, M., "Thermal conductance of metals in contact," *Proceedings of the General Discussion on Heat Transfer* (Institute of Mechanical Engineers, London, 1951), pp. 271–275.

[3] Laming, L. C., "Thermal conductance of machined metal contacts," *International Developments in Heat Transfer* (American Society of Mechanical Engineers, Boulder, Colo., 1961), pp. 65–76.

[4] Barzelay, M. E., Tong, K. N., and Holloway, G. F., "Effect of pressure on thermal conductance of contact joints," NACA TN 3295 (May 1955).

[5] Barzelay, M. E. and Holloway, G. F., "Interface thermal conductance of twenty-seven riveted aircraft joints," NACA TN 3991 (July 1957).

[6] Barzelay, M. E., "Range of interface thermal conductance for aircraft joints," NASA TN D-426 (May 1960).

[7] Barzelay, M. E. and Holloway, G. F., "Effect of an interface on transient temperature distribution in composite aircraft joints," NACA TN 3824 (April 1957).

[8] Barzelay, M. E., Tong, K. N., and Holloway, G. F., "Thermal conductance of contacts in aircraft joints," NACA TN 3167 (April 1954).

[9] Barzelay, M. E. and Schaefer, J. W., "Temperature profiles and interface thermal conductance of stainless steel and titanium alloy panels under combined loading and heating," Syracuse Univ. Research Rept. ME 406-577F (July 1957).

[10] Dusinberre, G. M., *Heat Transfer Calculations by Finite Differences* (International Textbook Co., Scranton, Pa., 1961), pp. 12–18.

[11] Almond, J. C. and Mikkelson, R. E., "Boeing thermal analyzer (Part 1, Engineering usage guide)," Boeing Doc. AS 0315, The Boeing Co., Seattle, Wash. (August 1964).

[12] Shlykof, Y. P., Ganin, E. A., and Demkin, N. B., "Analysis of contact heat exchange," Trans. Teploenerg. (Moscow) **7**, 72–76 (1960); English transl.; also Armed Services Technical Information Agency Doc. AD-429831.